

RESEARCH ARTICLE

OPEN ACCESS

Antimicrobial Activity and Confocal Microscopy of Bio-synthesized Titanium Nanoparticles from *Prosopis cineraria* Leaf Extract

Vaani Yadav*  and Varsha Gupta 

Department of Microbiology, Faculty of Science, JECRC University, Ramchandrapura Industrial Area, Vidhani, Sitapura Extension, Jaipur, Rajasthan, India.

Abstract

Nanoparticles offer exciting potential roles in targeted drug delivery mechanisms, allowing for precise and controlled release of medications into particular cells or tissues with minimal adverse effects. This study examined the antimicrobial activity of green-synthesised titanium nanoparticles from *Prosopis cineraria* leaf extract and determined their bactericidal properties by means of a live/dead assay. The bio-synthesized titanium dioxide (TiO_2) nanoparticles showed a peak at 20 values of 25.52° in X-ray diffraction, while scanning electron microscopy revealed it to be smooth and irregular in shape. Energy dispersive X-ray spectroscopy analysis of TiO_2 nanoparticles calcined at $550^\circ C$ confirmed the presence of only titanium and oxygen, with no detectable impurities. Atomic and weight percentages of titanium and oxygen were 23.54% and 47.96%, and 76.46% and 52.04%, respectively. The bio-synthesized TiO_2 nanoparticles was assessed for antimicrobial activity against bacterial strains and fungal isolates. The Titanium oxide, NPs exhibited effective antibacterial activity, with *Pseudomonas aeruginosa* showing the highest inhibition zone (13 mm), followed by *Escherichia coli* (12 mm), *Staphylococcus aureus* (11 mm), and *Bacillus subtilis* (9 mm) at a concentration of 80 μ l. For antifungal activity, the highest inhibition zone (17 mm) was observed against *Penicillium chrysogenum*, followed by *Candida albicans* (15 mm), *Aspergillus niger* (12 mm) and *Trichoderma reesei* (9 mm) at 80 μ l. The synthesised TiO_2 nanoparticles successfully inhibited the bacterial cells and showed green (live) and red (dead) fluorescence in the live/dead cell viability assay. The green-synthesised titanium NPs could inhibit bacterial and fungal growth, highlighting their potential use in biomedicine and healthcare.

Keywords: Antimicrobial Activity, Antibacterial, Antifungal, Confocal Microscopy, Live/Dead Assay, Titanium Nanoparticle

*Correspondence: pinki.21pmn002@jecrcu.edu.in

Citation: Yadav V, Gupta V. Antimicrobial Activity and Confocal Microscopy of Bio-synthesized Titanium Nanoparticles from *Prosopis cineraria* Leaf Extract. *J Pure Appl Microbiol.* 2025;19(4):2729-2744. doi: 10.22207/JPAM.19.4.09

© The Author(s) 2025. **Open Access.** This article is distributed under the terms of the [Creative Commons Attribution 4.0 International License](#) which permits unrestricted use, sharing, distribution, and reproduction in any medium, provided you give appropriate credit to the original author(s) and the source, provide a link to the Creative Commons license, and indicate if changes were made.

INTRODUCTION

Nanotechnology has gained considerable attention due to its transformative potential across diverse sectors such as electronic systems, renewable energy, environmental management, drug delivery, and bio-imaging.¹ In medicine, nanoparticles (NPs) have exhibited notable effectiveness in achieving targeted drug delivery by allowing controlled and precise drug release with minimal side effects.² Among the various approaches, the eco-conscious fabrication of nanoparticles using natural resources, such as plant extracts, offers an eco-friendly and sustainable method that has recently garnered increased interest.³ Metal NPs possess active surface sites that enhance their utility for drug delivery, analytical detection, and catalysis.⁴ Their unique characteristics render them valuable in various industries, including electronics, energy, medicine, and environmental technology.⁵

In particular, titanium dioxide (TiO_2) NPs are highly valued owing to their exceptional characteristics and versatile range of applications. In the biomedical sector, titanium's biocompatibility and corrosion resistance make it the preferred material for implants, such as joint replacements and dental devices.⁶ TiO_2 NPs can also enhance drug-loading efficiency and therapeutic outcomes in drug delivery systems⁷ and serve as effective catalysts owing to their reactive surface chemistry.⁸

Prosopis cineraria, also known as Khejri tree, has been studied for its antimicrobial properties, with its leaves and bark exhibiting significant antibacterial activity due to the involvement of flavonoids and tannins.⁹ Research has shown that distinct plant parts exhibit antibacterial effects against specific bacterial strains.¹⁰ This species plays a crucial ecological and medicinal role in arid regions of India, the Middle East and South Asia, offering benefits such as nitrogen fixation, soil stabilisation, and resistance to erosion.¹¹ The presence of phytochemicals—such as phenolic acids, flavonoids, and tannins—contributes to its antioxidant, antibacterial, anti-inflammatory, and antidiabetic properties.¹² Traditionally used in medicine, *P. cineraria* is known for treating numerous diseases and contains a wide spectrum of bioactive constituents, including proteins, saponins,

alkaloids, and terpenoids, supporting its potential for broader pharmacological applications.¹³ These findings highlight the importance of *P. cineraria* in traditional medicine and its potential applications in modern medicine and nutrition because of its antimicrobial properties. *P. cineraria* exhibits antimicrobial activity attributable to bioactive compounds present in its various parts, making it a valuable candidate for further research and potential utilisation in healthcare and nutrition.

The antimicrobial efficacy of green-synthesised NPs is often attributed to phytochemicals—such as flavonoids and alkaloids—present in the extracts of plants and used in their synthesis, as seen with *P. cineraria*, whose bioactive compounds impart antimicrobial properties to the resulting NPs.¹⁴ Silver NPs (AgNPs) formulated through *P. cineraria* have shown strong antibacterial activity against *Staphylococcus aureus* and *Escherichia coli*, owing to a combined mechanism of oxidative stress, membrane disruption, and inhibition of DNA replication.¹⁵ Studies on green synthesis using *P. cineraria* pod waste have confirmed the role of flavonoids and phenylpropanoids as reducing and capping agents, with Ag and silver copper NPs exhibiting strong antibacterial properties and up to 93% conversion efficiency in linalool epoxidation.¹⁶ Similarly, *Prosopis laevigata* extracts—rich in phenols, flavonoids, and alkaloids—have demonstrated potent antibacterial and antifungal effects *in vitro*.¹⁷ Alcoholic extracts from *P. cineraria* have also been effective against bacteria isolated from mastitis cows, with inhibition zones reaching 20.11 mm against *S. aureus*.¹⁸ In another case, silver oxide NPs synthesised using *P. cineraria* bark extract exhibited broad-spectrum antibacterial activity, as confirmed by scanning electron microscopy (SEM) analysis and X-ray diffraction (XRD).¹⁹

The use of *P. cineraria* in green nanotechnology shows promise in a range of applications owing to its capacity to enhance nanoparticle functionality. These NPs have been investigated for application in drug delivery systems, water purification, and antimicrobial coatings.²⁰ Their biocompatibility and stability make them suitable for carrying therapeutic agents to targeted tissues, while their antimicrobial properties support environmental applications

such as water decontamination.²¹ The TiO_2 NPs synthesised from *P. cineraria* extracts are especially valuable because of their ability to combat microbial infections and their relevance in the biomedical field. These nanoparticles exhibit strong antimicrobial efficacy against a broad spectrum of bacteria,²⁰ and have shown efficacy against therapy-resistant infectious agents such as *E. coli* and *S. aureus*, owing to their capability to disrupt cell membranes and instigate oxidative stress.²² Additionally, they possess antifungal potential, making them useful in treating infections and preventing microbial growth on medical devices.²³

In drug delivery, TiO_2 NPs derived from *P. cineraria* demonstrate robust structure with substantial drug-loading efficiency. The surface may be altered to facilitate targeted delivery, and the bioactive compounds from the plant aid in preserving NP stability in biological environments, reducing premature drug release.²⁴ These NPs can also be functionalised to bind specific receptors on tumour cells, enhancing delivery precision and enabling cancer therapy with minimal toxicity to healthy cells.²⁵ Beyond healthcare, TiO_2 NPs also have industrial and energy applications due to their strong photocatalytic properties. Dye-sensitised solar cells increase efficiency by boosting light absorption and facilitating better electron transport,²⁶ and the bioactive compounds in *P. cineraria* further boost their sensitising capabilities, contributing to environmentally friendly solar technologies.²⁷

In coatings, TiO_2 NPs provide antimicrobial and ultraviolet-blocking effects, making them suitable for textiles, packaging, and medical applications.²⁸ The bioactive compounds in *P. cineraria* contribute to improving the functionality of these coatings, ensuring long-term protection.²⁰ Moreover, green-synthesised NPs are increasingly applied in diagnostics and imaging. TiO_2 NPs obtained from *P. cineraria* have photo-luminescent properties, making them ideal as contrast agents for techniques such as fluorescence microscopy and magnetic resonance imaging, with minimal toxicity.²⁹ AgNPs synthesised from other plant extracts, such as *Moringa oleifera*, have also been incorporated into wound dressings, demonstrating strong antibacterial activity and promoting healing, offering a safe alternative to conventional

antimicrobial agents.³⁰ This study aimed to explore the green-synthesised titanium NP obtained from the leaf extract of *P. cineraria* and investigate their antimicrobial activities. The bactericidal property of the synthesised NP was also determined by using a live/dead cell viability assay.

Study objectives

- To synthesise TiO_2 NPs using a green synthesis method by employing a natural reducing and stabilising agent from the *P. cineraria* leaf extract.
- To characterise the synthesised TiO_2 NPs using techniques such as SEM, XRD, and energy dispersive X-ray spectroscopy (EDX) to determine their structural and elemental properties.
- To assess antimicrobial activity of bio-synthesised TiO_2 NPs against selected Gram-positive and Gram-negative bacterial strains, and fungal isolates.
- To evaluate the minimum inhibitory concentration (MIC) of TiO_2 NPs for both bacterial and fungal strains to assess their concentration-dependent antimicrobial effectiveness.
- To investigate the bactericidal effect of TiO_2 NPs using confocal laser scanning microscopy (CLSM) through live/dead cell viability assay.
- To explore the biomedical applications of *P. cineraria*-mediated TiO_2 NPs as eco-friendly and effective antimicrobial agents.

MATERIALS AND METHODS

Sample preparation

P. cineraria leaf powder (10 g) was mixed with 50 mL of distilled water to create a paste, then the supernatant was extracted by centrifugation, performed at 15,000 rpm for 15 min. Separately, 0.1 M titanium tetrakisopropoxide was added to 150 mL lukewarm purified water and sonicated for 20 min. The plant extract was gradually added to this solution, and colour changes were noted during magnetic stirring. After 24 h, the TiO_2 NPs were centrifuged, air-dried, and calcined at 550 °C for 4 h. Subsequently, the NPs were weighed and characterised using Fourier transform infrared spectroscopy, transmission electron microscopy, and ultraviolet-visible spectroscopy.

Characterisation

X-ray diffraction

XRD was performed on physiologically reduced silver-nitrate solutions drop-coated on glass slides using an X'Pert Pro diffractometer with the following specifications: Cu K α radiation, 40 kV, and 30 mA. The software utilised for the analysis was X'Pert HighScore Plus. The material to be analysed was finely ground and homogenised, and bulk composition and normal mass piece were obtained in accordance with the procedure.³¹ A thin layer of the produced AgNPs was placed on the XRD grid for investigation after they had been dried into a pellet.

Scanning electron microscopy

Operating at an extremely high tension or accelerating voltage of 20 kV, a SEM (Carl ZEISS EVOR-18, Germany) with a width of 8.5 mm was used to examine the real sizes and aggregation condition of the nanomaterial. Sample discs were loaded with minuscule amounts of the test ingredients one at a time. Before placing the materials on the specimen stage, sputter coating (gold coating) was applied to them using a Quorum Q150RS rotary pumped sputter coater to improve the image under a SEM.

Energy dispersive X-ray spectroscopy

Particles were separated through centrifugation of 20 ml of the sample suspension prepared in de-ionised water for 20 min at 10,000 rpm. The pellets were obtained and oven-dried at 50 °C to eliminate residual moisture. The dried powder sample was used for the EDX analysis. The titanium oxide NPs synthesised using leaf extract were dried and drop-coated onto a carbon film for the EDX examination. Hitachi S-3400 N SEM outfitted with a Thermo EDX detector was used for analysis.

Antimicrobial activity

The antibacterial properties of TiO₂ NPs were investigated *in vitro* using agar well diffusion method against bacterial strains Gram-positive *S. aureus* (MTCC 3381) and *Bacillus subtilis* (MTCC 10619), and Gram-negative *Pseudomonas aeruginosa* (MTCC 0424) and *E. coli* (MTCC 443).³² The antifungal activities were examined against *Trichoderma reesei* (MTCC 164), *Candida albicans* (MTCC 183), *Penicillium chrysogenum* (MTCC 5108), and *Aspergillus niger* (MTCC 872).

The bacterial medium was Mueller-Hinton agar No. 2 (Hi Media, India), and fungal media was Sabouraud's dextrose agar (Merck, Germany). Then, 20, 40, 60, and 80 μ L of plant-AgNPs were added for every 6 mm until the well was full. At 37 °C, the plates were incubated for the entire night. As antibacterial and antifungal medications, ciprofloxacin and ketoconazole were employed, respectively. For both bacterial and fungal species, the extract's antimicrobial spectrum was calculated using the zone size surrounding each well. Inhibition zone diameter of the agents were compared to those of the commercial control antibiotics.

Minimum inhibitory concentration

Using the method of agar well diffusion, the MIC of TiO₂ NPs were determined.³³ Strains of bacteria and fungi were sub-cultured in the appropriate culture media plates. In the wells of an agar plate, 30 μ L of the material was serially diluted twice using dimethyl sulfoxide (DMSO). Using sterile 0.9% saline water, a standardised inoculum (1.5×10^8 CFU/mL, 0.5 McFarland) was created. Using the seeded agar plates, wells were made. The 6 mm well was filled with varying concentrations of the PC-TiO₂ NPs solution. The plates were incubated for the whole night at 37 °C. Zone sizes surrounding each well were used to calculate the extract's antimicrobial spectrum against the bacterial species. The MIC of the extract for the tested microbiological species was determined by calculating the zone of inhibition with the smallest diameter that exhibited detectable growth inhibition. Each MIC test was conducted in triplicate.

Live/dead cell viability assay using confocal laser scanning microscopy

CLSM was employed to observe how bio-synthesized TiO₂ NPs interacted with *S. aureus*, *B. subtilis*, *E. coli*, and *P. aeruginosa*, aiming to evaluate their potential bactericidal activity. Following 12 and 24 h of incubation, the treated culture suspensions were collected by centrifugation (5000 rpm, 20 min). Phosphate-buffered saline was used to re-suspend the cell pellets. Acridine orange (5 mg/mL) and ethidium

bromide (3 mg/mL) were combined in equal amounts in ethanol to create the staining solution. After mixing 10 μ L of the re-suspended solution with 20 μ L of the staining solution for 15 min, the mixture was incubated at 37 °C. The final step in the procedure was mixing acridine orange (4 μ L) and ethidium bromide (6 μ L) staining dyes individually with 100 μ L of each bacterium pellet, which were then incubated for 15 min at 37 °C. Prior to being examined using CLSM, clear glass slides were used to hold the prepared test bacterial samples.³⁴

Statistical analysis

Three duplicates of each treatment were carried out, and the mean \pm standard error (SE) was used to present the data.

$$SE = SD / \sqrt{N}$$

Here, SD = standard deviation

N = no. of observations or sample sizes

RESULT AND DISCUSSION

The manufacture of titanium NPs from *P. cineraria* leaf extract is described in this paper. Water was used as the solvent for producing the

leaf extract. The leaf extract was incorporated into a titanium isopropoxide solution, which caused the solution's colour to change noticeably from yellow to orange. This orange hue demonstrated that titanium isopropoxide had been successfully reduced to TiO_2 NPs. The white hue of TiO_2 NPs was obtained by calcining the manufactured NP in a muffle furnace. Following production, the NPs were thoroughly characterised using XRD, SEM, and EDX analysis.

Characterisation of Titanium nanoparticle X-ray diffraction

XRD is widely implemented in NP characterisation due to its ability to offer insights into crystal structure, dimensions and nanoparticle formulation. In this study, the crystallinity and phase of the prepared TiO_2 NPs were analysed using XRD and the peaks were observed at 2θ values of 25.52°, 38.17°, 48.38°, 54.22°, 55.17° and 63.03°. The sharpest narrow peak of the sample was identified by 2θ , which confirmed an anatase structure at $2\theta = 25.52^\circ$ (Figure 1). Similarly, green-synthesised TiO_2 NP from the capping agent *Erythrina variegata* leaf aqueous extract was analysed, where the XRD results confirmed

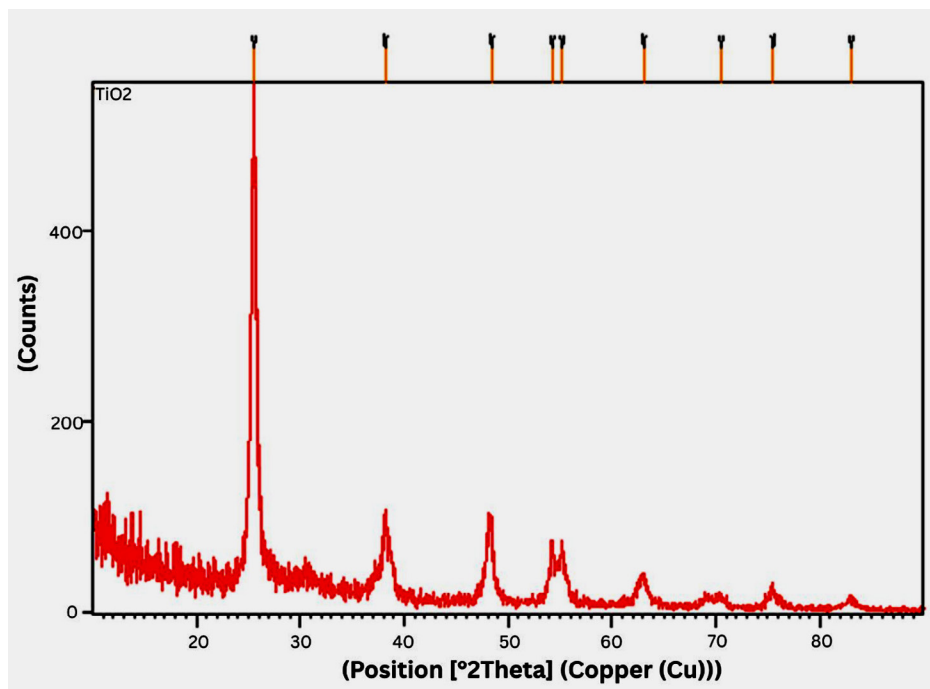


Figure 1. X-ray diffraction graph of synthesised titanium dioxide nanoparticles

the structural characteristics of the synthesised TiO_2 NPs by showing various peaks. The maximum peak appeared at 2θ value of 25.28° , which corresponds to an average size of TiO_2 of 7.91 nm .³⁵ Also another study aimed for the formation of (TiO_2) NPs using *Luffa acutangula* leaf extract and characterised the nanoparticle structure using XRD analysis where the diffraction angle (2θ) were observed at 25.47° (101), 28.30° (110), 29.51°

(222), 31.65° (100), 40.42° (111), 48.98° (200) and 54.69° (105), respectively indicating the crystalline structure of nanoparticle.³⁶ The synthesised titanium oxide NP from *Pouteria campechiana* leaf extract, as analysed by the XRD pattern, obtained diffraction peaks for 110, 101, 111, 210, and 211, indicating the structural configuration of the crystal in the nanoparticle.³⁷

Table 1. Antibacterial activity of titanium nanoparticles synthesized from *Prosopis cineraria* leaf extract

Bacteria	Standard	Inhibition zone (mm)			
		20 μl	40 μl	60 μl	80 μl
Gram-positive	<i>Staphylococcus aureus</i>	30	7 \pm 0.23	8 \pm 1.52	10 \pm 0.67
	<i>Bacillus subtilis</i>	30	Nil	Nil	7 \pm 0.15
Gram-negative	<i>Escherichia coli</i>	30	Nil	10 \pm 0.48	11 \pm 1.51
	<i>Pseudomonas aeruginosa</i>	30	9 \pm 0.74	9 \pm 1.61	10 \pm 2.15
					13 \pm 0.45

Table 2. Antifungal activity of synthesized titanium nanoparticles from *Prosopis cineraria* leaf extract

Fungi	Standard	Inhibition zone (mm)			
		20 μl	40 μl	60 μl	80 μl
<i>Candida albicans</i>	40	11 \pm 0.51	12 \pm 1.23	13 \pm 0.94	15 \pm 2.06
<i>Trichoderma reesei</i>	40	Nil	Nil	Nil	9 \pm 0.97
<i>Penicillium chrysogenum</i>	40	11 \pm 0.35	14 \pm 1.07	15 \pm 0.15	17 \pm 1.48
<i>Aspergillus flavus</i>	40	Nil	Nil	9 \pm 0.64	12 \pm 1.94

Table 3. Minimum bacterial inhibitory concentration of synthesized titanium nanoparticles

Bacterial strain	Concentration (mg) \pm standard error of mean
<i>Staphylococcus aureus</i>	200 \pm 1.02
<i>Bacillus subtilis</i>	600 \pm 0.95
<i>Escherichia coli</i>	300 \pm 1.13
<i>Pseudomonas aeruginosa</i>	100 \pm 0.51

Table 4. Minimum fungal inhibitory concentration of synthesized titanium nanoparticles

Fungal strain	Concentration (mg) \pm standard error of mean
<i>Candida albicans</i>	100 \pm 0.12
<i>Trichoderma reesei</i>	700 \pm 0.94
<i>Penicillium chrysogenum</i>	100 \pm 1.23
<i>Aspergillus flavus</i>	550 \pm 0.75

Scanning electron microscopy

High-resolution topographic images and surface morphology of NPs can be obtained using SEM. In this study, green-generated TiO_2 NPs from *P. cineraria* leaves were measured using SEM images, and topographical analysis was performed based on a surface study, which revealed that the synthesised TiO_2 NPs were smooth and irregular in shape (Figure 2). In another study, TiO_2 NPs were generated from the aqueous extract of *E. variegata* leaves, and SEM analysis was used to evaluate the morphological aspects of the TiO_2

NPs.³⁵ The synthesised TiO_2 NP was verified by the SEM. The size and shape of the titanium oxide NP, synthesised from *P. campechiana* leaf extract, was studied through SEM analysis and the size ranged 73-140 nm with a polydisperse structure.³⁷ White TiO_2 NPs were created using an extract from *Azadirachta indica*. The size and surface morphology of the NPs were examined using SEM, which showed that they were spherical and ranged 25-87 nm in size.³⁸ Greenly produced TiO_2 NPs were prepared from *Mentha arvensis* leaf extract. Their size, surface characteristics,

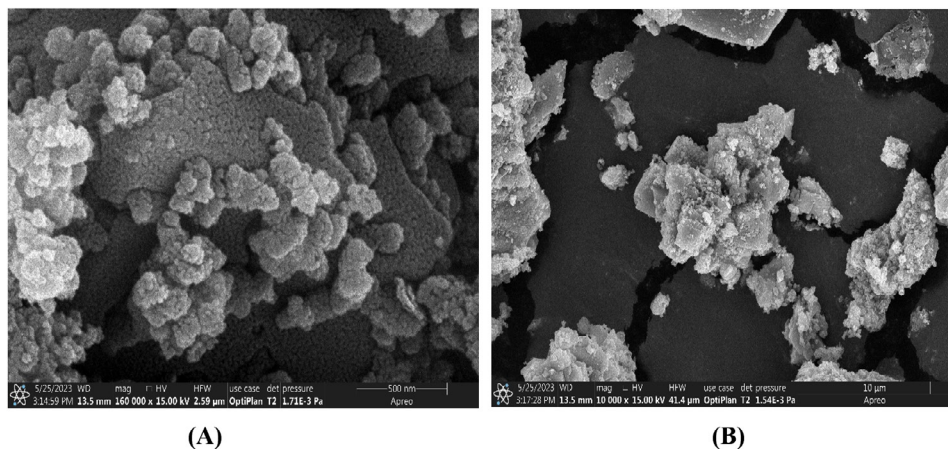


Figure 2. Scanning electron microscopy micrographs of synthesized titanium dioxide nanoparticles from a scale size of (A) 500 nm, and (B) 10 μm

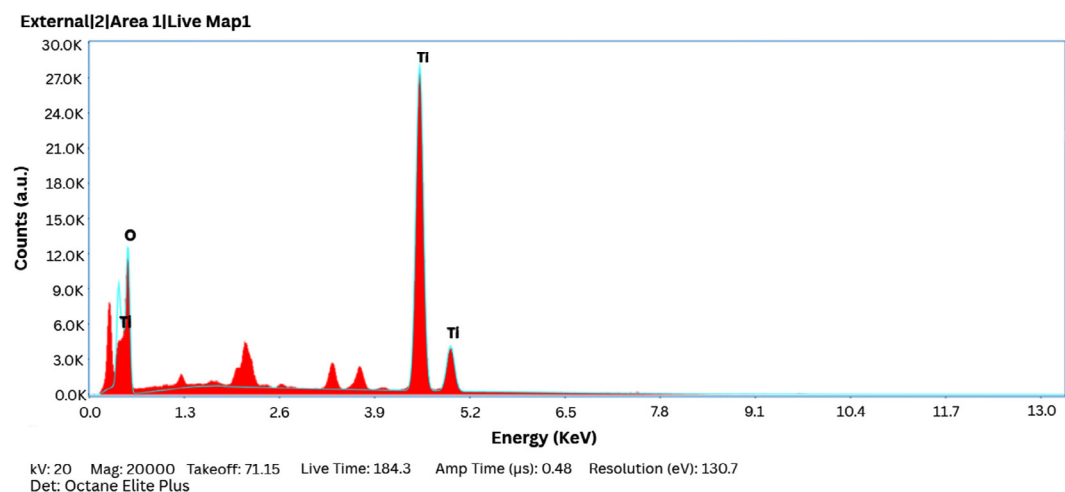


Figure 3. Energy dispersive X-ray spectrometry graph of synthesized titanium dioxide nanoparticles

and shape were examined using SEM, revealing an average size of 20–70 nm, uniform distribution, smooth, and spherical in shape, respectively.³⁹

Energy dispersive X-ray spectrometry

EDX determination of titanium and oxygen showed peaks of TiO_2 NPs at 550 °C. No other contaminants were detected within the

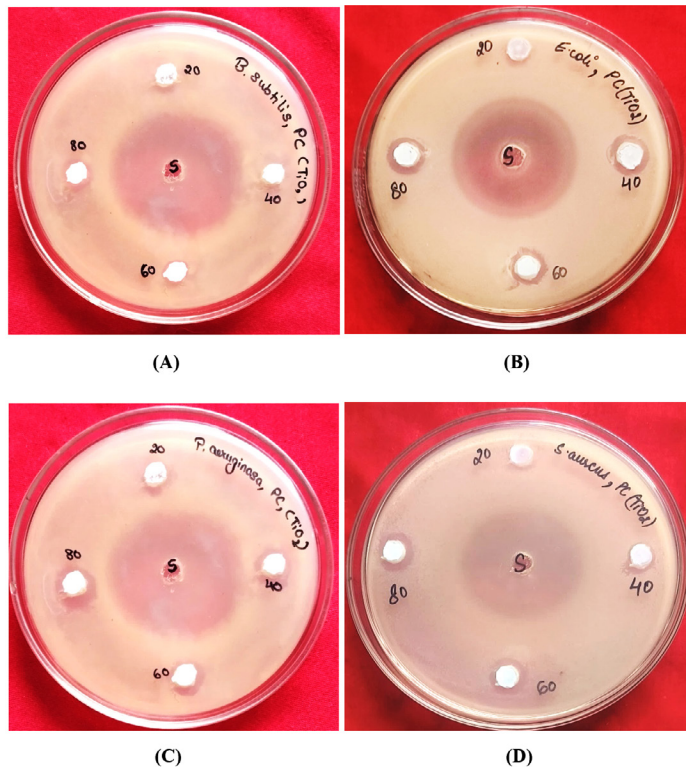


Figure 4. Antibacterial activity of titanium nanoparticles against (A) *Bacillus subtilis*, (B) *Escherichia coli*, (C) *Pseudomonas aeruginosa*, and (D) *Staphylococcus aureus*

Antibacterial Activity

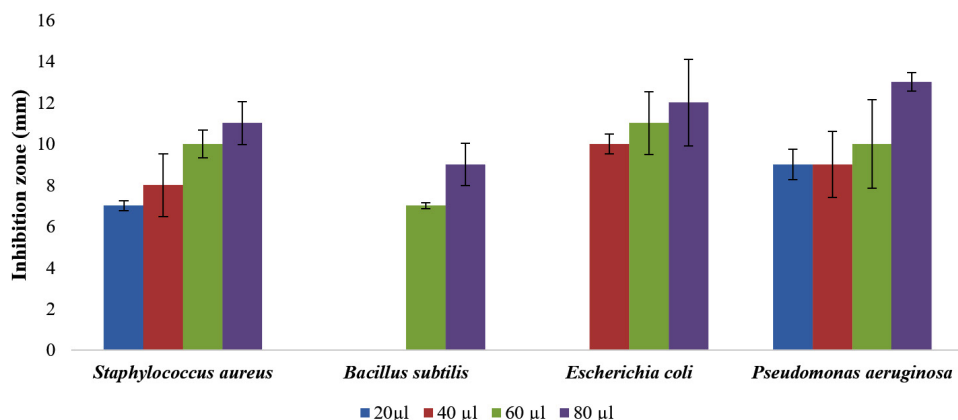


Figure 5. Antibacterial activity of titanium nanoparticles against *Staphylococcus aureus*, *Bacillus subtilis*, *Escherichia coli*, and *Pseudomonas aeruginosa*

EDX detection range. The titanium and oxygen atomic percentages were 23.54% and 76.46%, respectively, whereas the weight percentages were 47.96% and 52.04%, respectively (Figure 3). EDX-used for elemental makeup analysis of NPs is frequently combined with SEM or transmission

electron microscopy. When exposed to an electron beam, it detects the distinctive X-rays that the components in the sample release. The EDX spectra provide qualitative and quantitative information on the chemical elements present in the NPs. This technique helps determine the

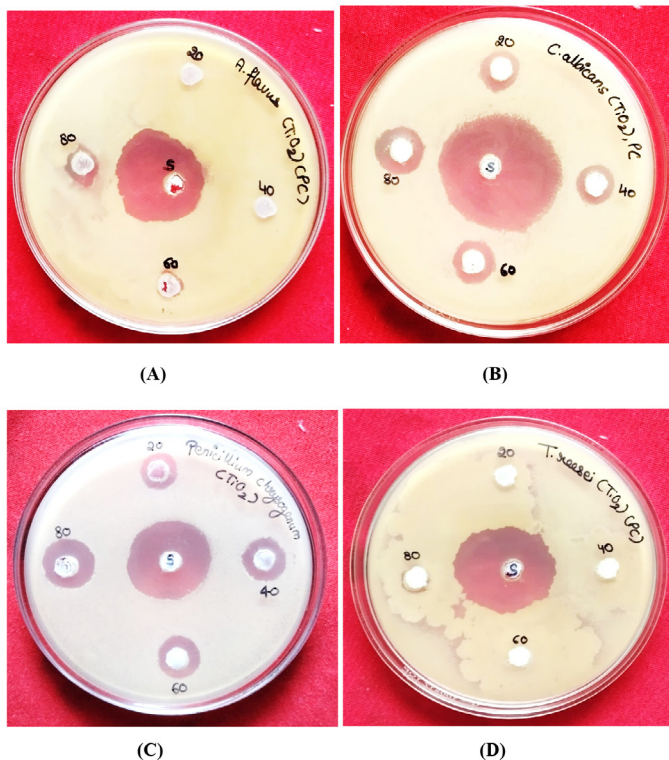


Figure 6. Antifungal activity of titanium nanoparticle against (A) *Aspergillus flavus*, (B) *Candida albicans*, (C) *Penicillium chrysogenum*, and (D) *Trichoderma reesei*

Antifungal Activity

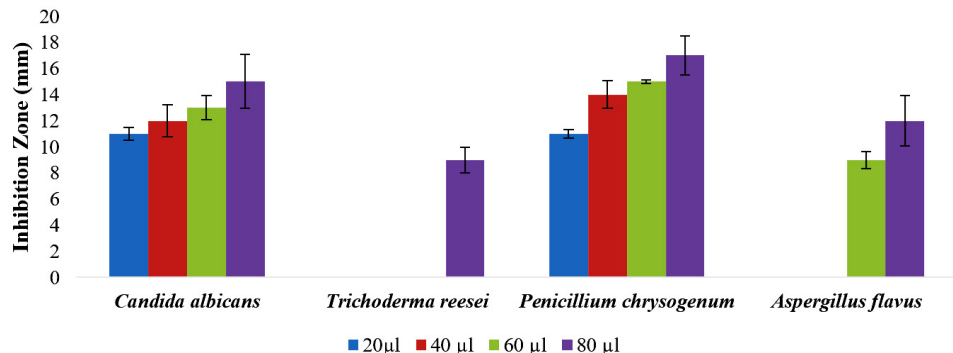


Figure 7. Antifungal activity of titanium nanoparticles against *Candida albicans*, *Trichoderma reesei*, *Penicillium chrysogenum*, and *Aspergillus flavus*

elemental composition, identify impurities, and study the elemental distribution within the NPs. EDX mapping can provide spatial information on the distribution of elements at the nanoscale level. Since no traces of any other impurities could be detected within the EDX detection limit, the current study's EDX analysis of TiO_2 NPs at 550 °C reveals peaks for titanium and oxygen.

Similarly, TiO_2 NPs that were greenly produced from the aqueous extract of *E. variegata* leaves were examined in the TiO_2 EDX spectrum, which revealed peaks for the elements titanium, oxygen, and carbon.³⁵ They concluded that the existence of minerals in the *E. variegata* extract were the cause for the observed carbon peak. Titanium NPs were bio-synthesized from

Trigonella foenum-graecum's aqueous leaf extract, and the presence of various elements was verified using EDX spectra, which showed the existence of titanium and oxygen molecules at a peak of 0.452 keV and 0.525 keV.⁴⁰ Additionally, another study used *L. acutangula* leaf extract to synthesise TiO_2 NPs and used EDX to identify the components of TiO_2 NPs. Around 0.5 and 0.6, peaks were discovered, which were associated with the binding energies of titanium and oxygen.³⁶ In synthesised titanium oxide NP from *P. campechiana* leaf extract, and the EDX spectrum results revealed the presence of elements such as titanium and oxygen in the major portion, and in minor states, the elements such as calcium, magnesium, and aluminium were also analysed.³⁷

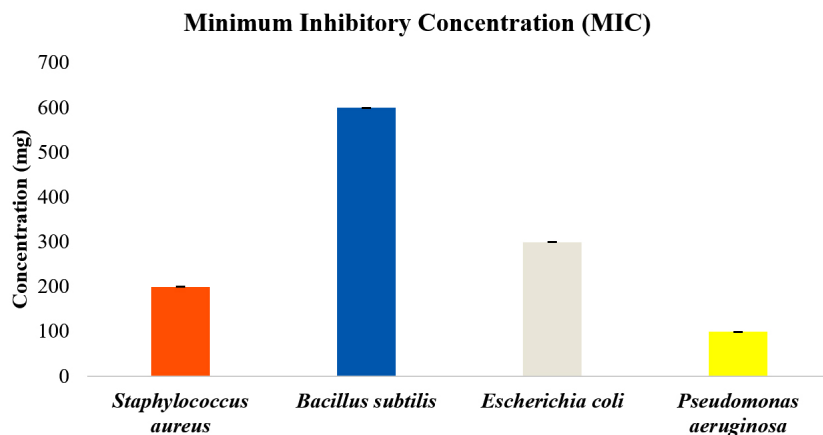


Figure 8. Minimum bacterial inhibitory concentration of synthesized titanium nanoparticles

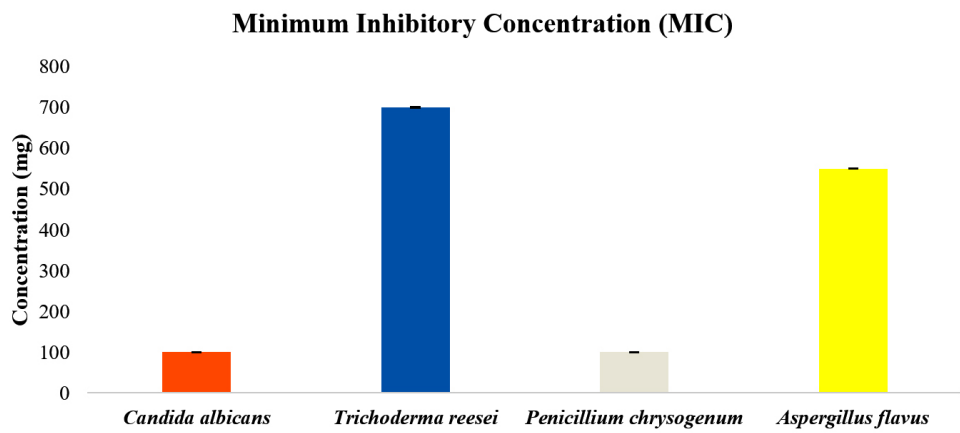


Figure 9. Minimum fungal inhibitory concentration of synthesized titanium nanoparticles

Antimicrobial activity

Antibacterial activity

The significance of the antimicrobial properties of bio-synthesized NPs is multifaceted and has broad implications in various fields. bio-synthesized NPs have demonstrated antibacterial activity, offering a potential alternative to traditional antibiotics. This is especially significant in the context of antibiotic resistance, as NPs

may combat drug-resistant bacterial strains.⁴¹ In the present work, antibacterial activity of green-synthesised titanium NP was studied (Table 1), and the results revealed successful inhibition of *P. aeruginosa*, *E. coli*, *B. subtilis*, and *S. aureus* growth with maximum inhibition of 10 mm against *E. coli* at 40 μ l concentration. However, the maximal zone of inhibition was recorded against *P. aeruginosa* (13 mm) at 80 μ l (Figures 4 and 5).

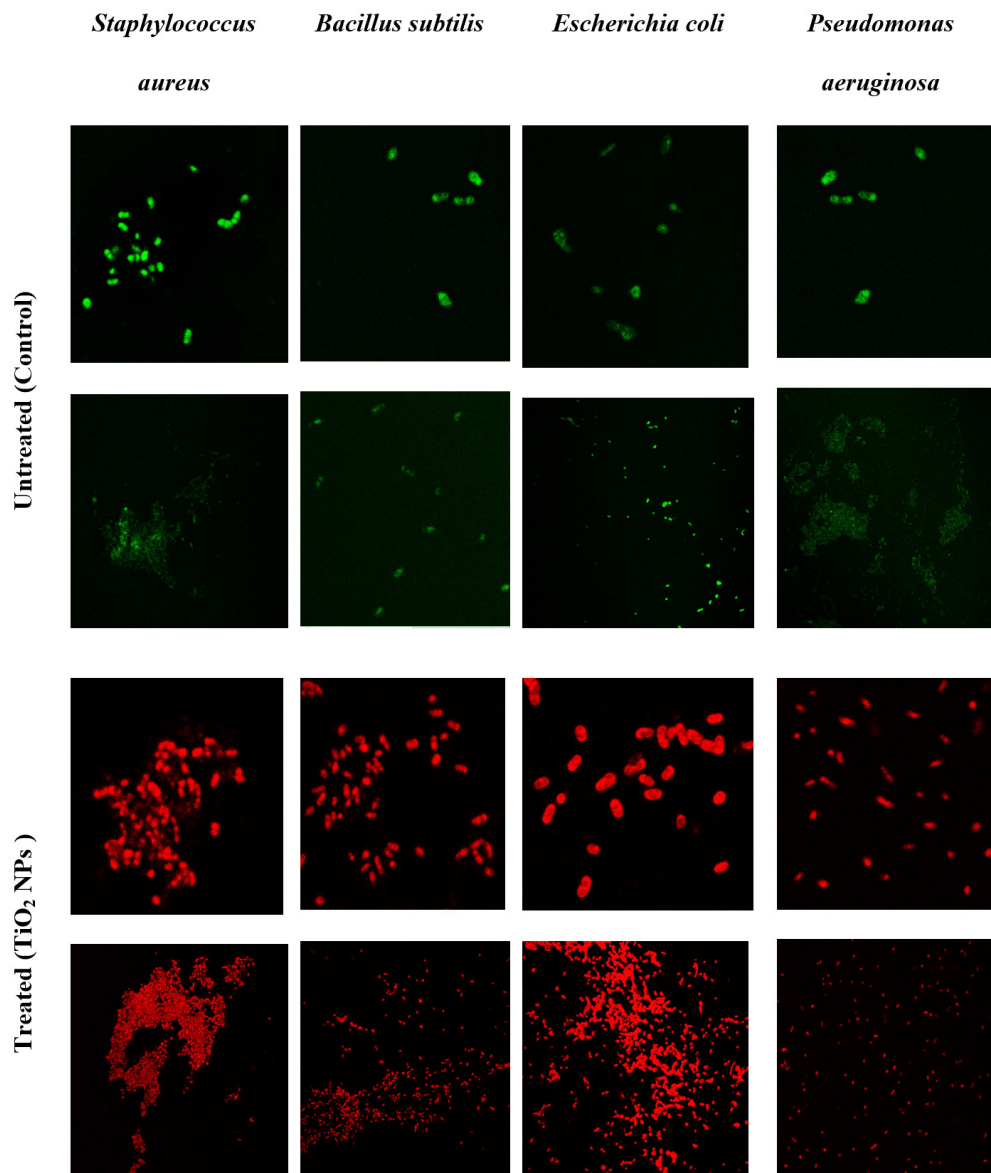


Figure 10. Confocal laser scanning microscopic images of bio-synthesized titanium dioxide nanoparticles treated and untreated pathogenic bacterial cells of *Staphylococcus aureus*, *Bacillus subtilis*, *Escherichia coli*, and *Pseudomonas aeruginosa*

The well diffusion method was used similarly to assess *in vitro* antibacterial efficacy of *P. cineraria* methanolic bark extract against multidrug-resistant *P. aeruginosa*, *E. coli*, *K. pneumonia*, and *S. aureus*. The controls, both positive and negative, were the medicines DMSO and tetracycline, respectively. The crude extract yield as a percentage was 7.9%. When antimicrobial efficiency was assessed and compared with the common antibiotic tetracycline, the bark extract was remarkably potent against *S. aureus* and *E. coli*.⁴² The TiO_2 NPs derived from *E. variegata* aqueous extract were also investigated. Green-synthesised TiO_2 NPs' antibacterial activity was investigated against four distinct pathogenic strains: *Streptococcus*, *Staphylococcus*, *P. aeruginosa*, and *E. coli*. The zones of inhibition for Gram-positive and Gram-negative bacteria were determined to be 7, 2, 8, and 14 mm using the disk diffusion method. According to the findings, TiO_2 NPs made from *E. variegata* leaves had the strongest antibacterial activity against *P. aeruginosa*.³⁵

Antifungal activity

The synthesised NPs antifungal activity is significant because of their potential as alternative antifungal agents, applicability in biomedicine, role in enhancing existing antifungal treatments, eco-friendly applications, and contribution to ongoing scientific advancements. NPs can also be used in agriculture and in the environment to combat fungal pathogens that affect crops and ecosystems. They offer an eco-friendly approach to control fungal diseases.⁴³ As a result, the current study examined the synthetic titanium NPs' antifungal activity (Table 2). The findings showed that the growth of *P. chrysogenum*, *C. albicans*, *T. reesei*, and *A. niger* was inhibited by a maximal inhibition zone of 11 mm against *P. chrysogenum* and *C. albicans* at 20 μl . At a dose of 80 μl , the greatest inhibition zone of 17 mm was seen against *P. chrysogenum* (Figures 6 and 7).

The antifungal properties of *Mentha arvensis* leaf extract were evaluated using disc diffusion approaches in greenly produced titanium dioxide NPs against *A. cuboid*, *A. fumigatus*, and *A. niger*. *A. niger* was significantly inhibited by the produced TiO_2 NPs. However, against other

chosen pathogens, the NPs had no evident antifungal action.³⁹ A study used a green strategy for the biocontrol of fungal strains, focusing on biosynthesising TiO_2 NPs. They identified 19 fungal strains, including *Aspergillus* and *Penicillium* species. The findings demonstrated that TiO_2 NPs efficiently and dose-dependently suppressed fungal growth at doses of 300, 200, and 100 $\mu\text{g}/\text{mL}$, with varying inhibition zones.⁴⁴ However, a few reports have been found on the antifungal activity of green-synthesised titanium NP and *P. cineraria*. This study is therefore the first to investigate the antifungal activity of *P. cineraria* and green-synthesised titanium NP.

Minimum inhibitory concentration

The MIC analysis of bio-synthesized NPs is a critical method used in microbiology and nanotechnology research. The bio-synthesized NPs efficiency in stopping the bacterial growth was evaluated with the aid of MIC analysis. It indicates the antimicrobial qualities of the NPs by quantitatively measuring the minimal dose needed to suppress bacterial development.⁴⁵ The MIC of the generated TiO_2 in this investigation was determined, in which the results indicated that *P. aeruginosa* showed minimum inhibition at 100 mg concentration (Figure 8 and Table 3). However, *C. albicans* and *P. chrysogenum* exhibited minimal inhibition at 100 mg concentration of titanium NPs (Figure 9 and Table 4). A study examined the antibacterial qualities of TiO_2 quantum dots (TiO_2 Qds) produced by biosynthesising them using watermelon peel waste in an environmentally friendly manner. For *B. subtilis*, *E. coli*, *C. neoformans*, *C. albicans*, *A. niger*, and *A. fumigatus*, the TiO_2 Qds showed potent antibacterial action, with (MICs) of 15.62, 62.5, 7.81, 7.81, 31.25, and 1.95 $\mu\text{g}/\text{mL}$, respectively.⁴⁶ A study evaluated the antimicrobial properties of TiO_2 NPs and investigated their environmentally friendly green synthesis using leaf extract from *J. phoenicea*, and found them to be effective against *A. niger*, *E. coli*, *B. subtilis*, *S. aureus*, *P. digitatum*, *S. cerevisiae*, and *K. pneumoniae*. The inhibition zones for *K. pneumoniae* and *A. niger* ranged 15.7-30.3 mm, respectively. The lowest MIC was 20 $\mu\text{L}/\text{mL}$ and the lowest minimum bacterial inhibitory concentration was 40 $\mu\text{L}/\text{mL}$ against *A. niger*.⁴⁷

Live/dead cell viability assay using confocal microscopy

Confocal microscopy is a powerful imaging technique widely used in cell biology and life sciences to assess live/dead cell viability. This method allows for high-resolution, three-dimensional visualisation of cells and tissues, making it particularly valuable for studying the dynamics of investigated living cells.⁴⁸ The present study examined the bactericidal properties of eco-friendly synthesised TiO_2 NPs by treating pathogenic bacteria of Gram-negative (*E. coli* and *P. aeruginosa*) and Gram-positive (*S. aureus* and *B. subtilis*) strains. CLSM was used to visually inspect the bacterial survival and cell membrane interaction of these bacteria following treatment with ethidium bromide and acridine orange dyes. The treated bacterial cells were red in colour (dead) and untreated bacterial cell membranes were green in colour (live) in the confocal microscopy images. The best results were observed for dangerous bacteria *E. coli* and *P. aeruginosa* with the high killing efficacy of synthesised TiO_2 NPs against them attributed to phytochemical-mediated TiO_2 NP synthesis (Figure 10).

In a study comparing *Streptococcus pneumoniae* and *Staphylococcus epidermidis*, bio-synthesized NPs utilising the leaf extract of *Psidium guajava* showed the strongest antibacterial efficacy against *E. coli* and *P. aeruginosa*. CLSM, which visualises both living and dead bacterial cells was used to confirm the interaction of NPs with the bacterial membranes. The phytochemical-mediated synthesis was responsible for the remarkable killing efficacy of NPs against harmful bacteria.³⁴

Another study used CLSM to investigate the activity and interaction against human infections of AgNPs synthesised from *Aloe arborescens* leaf extract. According to the findings, AgNPs causes bacterial cell death by damaging the cellular membranes of *S. aureus* and *P. aeruginosa*.⁴⁹ In drug delivery research, the live/dead assay is used to assess the effectiveness of NPs with drug delivery systems and their impact on target cells.⁵⁰ However, no studies have been conducted on the live/dead assay of green-synthesised titanium NP and *P. cineraria* using confocal microscopy. This is the first study

to utilise the live/dead assay of *P. cineraria* and green-synthesised titanium NPs.

CONCLUSION

The antimicrobial properties of titanium NPs prepared from the extract of *P. cineraria* leaves were explored. The successful synthesis of nanoparticle was achieved through XRD and SEM analysis in which the nanoparticle showed a peak at 2θ values of 25.52° in XRD, while SEM analysis showed that the synthesised TiO_2 NPs were smooth and irregular in shape. EDX confirmed the composition of the elements of TiO_2 NPs, with titanium and oxygen as the primary elements. When the produced titanium NPs were tested for antibacterial properties, the TiO_2 NPs effectively stopped the development of *B. subtilis*, *P. aeruginosa*, *S. aureus*, and *E. coli*. The NPs effectively inhibited the growth of *A. niger*, *C. albicans*, *P. chrysogenum*, and *T. reesei* in the case of antifungal activity. In the live/dead cell viability assay, the synthesised titanium NPs successfully inhibited the bacterial cells and showed green (live) and red (dead) fluorescence. From the results of this study, it can be demonstrated that the titanium NPs synthesised from *P. cineraria* have the potential to inhibit bacterial and fungal growth and can be used effectively in the biomedical and health care sectors in the future.

ACKNOWLEDGMENTS

The authors are thankful to the Department of Microbiology, JECRC University, for providing the related support to compile this work.

CONFLICT OF INTEREST

The authors declare that there is no conflict of interest.

AUTHORS' CONTRIBUTION

VY performed the experiments, analyzed the data, and drafted the manuscript. VG supervised the study. Both authors read and approved the final manuscript for publication.

FUNDING

None.

DATA AVAILABILITY

All datasets generated or analyzed during this study are included in the manuscript.

ETHICS STATEMENT

This article does not contain any studies with human participants or animals performed by any of the authors.

REFERENCES

1. Barrios E, Fox D, Li Sip YY, et al. Nanomaterials in advanced, high-performance aerogel composites: A review. *Polymers.* 2019;11(4):726. doi: 10.3390/polym11040726
2. Singh KR, Nayak V, Singh J, Singh AK, Singh RP. Potentialities of bioinspired metal and metal oxide NPs in biomedical sciences. *RSC Adv.* 2021;11(40):24722-24746. doi: 10.1039/DRA04273D
3. Vashisth N, Sharma SP, Kumar S, Yadav A. Green synthesis of 3-(1-naphthyl), 4-methyl-3-(1-naphthyl) coumarins and 3-phenylcoumarins using dual-frequency ultrasonication. *Green Processing and Synthesis.* 2020;9(1):399-404. doi: 10.1515/gps-2020-0042
4. Long R, Li Y, Song L, Xiong Y. Coupling solar energy into reactions: Materials design for surface plasmon-mediated catalysis. *Small.* 2015;11(32):3873-3889. doi: 10.1002/smll.201403777
5. Pareek V, Bhargava A, Gupta R, Jain N, Panwar J. Synthesis and applications of noble metal NPs: A review. *Adv Sci Eng Med.* 2017;9(7):527-544. doi: 10.1166/asem.2017.2027
6. Kulkarni M, Mazare A, Gongadze E, et al. Titanium nanostructures for biomedical applications. *Nanotechnology.* 2015;26(6):062002. doi: 10.1088/0957-4484/26/6/062002
7. Patra JK, Das G, Fraceto LF, et al. Nano based drug delivery systems: Recent developments and future prospects. *J Nanobiotechnol.* 2018;16(1):1-33. doi: 10.1186/s12951-018-0392-8
8. Lin H, Chen Y, Shi J. Nanoparticle-triggered *in situ* catalytic chemical reactions for tumour-specific therapy. *Chem Soc Rev.* 2018;47(6):1938-1958. doi: 10.1039/C7CS00471K
9. Afifi HSA, Al-rub IA. *Prosopis cineraria* as an unconventional legume: Nutrition and health benefits. In: Legume Seed Nutraceutical Research. IntechOpen. 2018. doi: 10.5772/intechopen.79291
10. Khokar A, Menghani E. Antimicrobial activity of *Prosopis cineraria* (leaf) methanol and chloroform extract against selected bacterial species. *Int J Pharm Biol Sci.* 2015;6(3):B222-B229.
11. Sharma M, Singh CP. Functional genomics of *Prosopis cineraria* (L.) Druce: Recent advances and new prospects. *J Plant Biochem Biotechnol.* 2025;34(1):1-17. doi: 10.1007/s13562-024-00948-3
12. Sharma V, Anand S, Choubey S, Shahi S. *Prosopis cineraria*: A desert treasure trove of bioactive compounds. *Cuestiones de Fisioterapia.* 2024;53(3):538-544. doi: 10.48047/652m4m57
13. Pandey V, Patel S, Danai P, Yadav G, Kumar A. Phytoconstituents profiling of *Prosopis cineraria* and in vitro assessment of antioxidant and anti-ulcerogenicity activities. *Phytomedicine Plus.* 2023;3(3):100452. doi: 10.1016/j.phyplu.2023.100452
14. Chowdhury A, Ara J, Islam MS. Green synthesis of phytochemical nanoparticles and their antimicrobial activity: a review study. *Biomed J Sci Tech Res.* 2021;34(4):26929-26935. doi: 10.26717/BJSTR.2021.34.005580
15. Ishwarya R, Vaseeharan B, Kalyani S, et al. Facile green synthesis of zinc oxide nanoparticles using *Ulva lactuca* seaweed extract and evaluation of their photocatalytic, antibiofilm and insecticidal activity. *J Photochem Photobiol B.* 2018;178:249-258. doi: 10.1016/j.jphotobiol.2017.11.006
16. Kumar P, Sharma PK, Chaturvedi S, et al. Green production of biologically active Ag and Ag-Cu NPs from *Prosopis cineraria* pod waste extract and their application in epoxidation. *Res Chem Intermed.* 2023;49(105):557-575. doi: 10.1007/s11164-022-04887-3
17. Nava-Solis U, Rodriguez-Canales M, Hernandez-Hernandez AB, et al. Antimicrobial activity of the methanolic leaf extract of *Prosopis laevigata*. *Sci Rep.* 2022;12(1):20807. doi: 10.1038/s41598-022-25271-6
18. Savitha, Singh AP, Nayak TC, Kachhawa JP, Gupta SR, Tanwar RK. Antibacterial efficacy of alcoholic extract of leaves and bark of *Prosopis cineraria* against common bacterial isolates from subclinical mastitis affected cows. *Veterinary Practitioner.* 2024;25(1):6-11.
19. Kalaivani P, Mathubala G. Green synthesis of AgO NPs using *Prosopis cineraria* bark extract and its antibacterial activity. *J Phys Conf Ser.* 2024;2886(1):012001. doi: 10.1088/1742-6596/2886/1/012001
20. Ahmed S, Ahmad M, Swami BL, Ikram S. A review on plant extract mediated synthesis of silver NPs for antimicrobial applications: A green expertise. *J Adv Res.* 2016;7(1):17-28. doi: 10.1016/j.jare.2015.02.007
21. Alkaabi DS, Gasimelbari ME, Abumukhaimar NAH, Ibrahim MAFS. Antimicrobial activity of United Arab Emirates indigenous medicinal plants *Prosopis cineraria*, *Prosopis juliflora* and *Acacia tortilis*. *Hamdan Medical Journal.* 2020;13(2):110-114. doi: 10.4103/HMJ.HMJ_82_19
22. Jinu U, Gomathi M, Saiqa I, Geetha N, Benelli G, Venkatachalam P. Green engineered biomolecule-capped silver and copper nanohybrids using *Prosopis cineraria* leaf extract: Enhanced antibacterial activity against microbial pathogens of public health relevance and cytotoxicity on human breast cancer cells (MCF-7). *Microbial Pathogenesis.* 2017;105:86-95. doi: 10.1016/j.micpath.2017.02.019
23. Upadhyay TK, Mathur M, Prajapat RK, Nagar SK, Singh K, Khan F, Pandey P, Khan MM. *Prosopis cineraria* (Khejri): Ethnopharmacology and phytochemistry. In: Sharangi AB, Peter KV eds. *Medicinal Plants.* Apple Academic Press; 2022. 409-423. doi: 10.1201/9781003189966-23
24. Mittal AK, Chisti Y, Banerjee UC. Synthesis of metallic NPs

using plant extracts. *Biotechnol Adv.* 2016;31(2):346-356. doi: 10.1016/j.biotechadv.2013.01.003

25. Pavithra S, Bessy TC, Bindhu MR, et al. Photocatalytic and photovoltaic applications of green synthesized titanium oxide (TiO_2) nanoparticles by *Calotropis gigantea* extract. *Alloys Compd.* 2023;960:170638. doi: 10.1016/j.jallcom.2023.170638

26. Munir H, Bilal M, Mulla SI, Abbas Khan H, Iqbal HMN. Plant-mediated green synthesis of nanoparticles. In: Inamuddin, Boddu R, Ahmed MI, Khan A. (eds) *Advances in Green Synthesis. Advances in Science, Technology & Innovation*. Springer, Cham. 2021:75-89. doi: 10.1007/978-3-030-67884-5_5

27. Singh AP, Biswas A, Shukla A, Maiti P. Targeted therapy in chronic diseases using nanomaterial-based drug delivery vehicles. *Signal Transduct Target Ther.* 2019;4(1):33. doi: 10.1038/s41392-019-0068-3

28. Mahlambi MM, Ngila CJ, Mamba BB. Recent developments in environmental photocatalytic degradation of organic pollutants: The case of titanium dioxide nanoparticles—a review. *J Nanomater.* 2015;2015(1):790173. doi: 10.1155/2015/790173

29. Ajay S, Panicker JS, Manjumol KA, Subramanian PP. Photocatalytic activity of biogenic silver NPs synthesized using *Coleus Vettiveroids*. *Inorg Chem Commun.* 2022;144:109926. doi: 10.1016/j.inoche.2022.109926

30. Mousa SA, Shalan AE, Hassan HH, Ebnawaled AA, Khairy SA. Enhanced photocatalytic degradation of titanium dioxide nanoparticles synthesized by different plant extracts for wastewater treatment. *J Mole Struct.* 2022;1250:131912. doi: 10.1016/j.molstruc.2021.131912

31. Dimitrijevic R, Cvetkovic O, Miodragovic Z, Simic M, Manojlovic D, Jovic V. SEM/EDX and XRD characterization of silver nanocrystalline thin film prepared from organometallic solution precursor. *J Min Metall Sect B-Metall.* 2013;49(1):91-95.

32. Perez C, Paul M, Bazerque P. An antibiotic assay by the agar-well diffusion method. *Acta Biologica Medica Experimental.* 1990;15:113-115.

33. Wiegand I, Hilpert K, Hancock REW. Agar and broth dilution methods to determine the minimal inhibitory concentration (MIC) of antimicrobial substances. *Nature Protocols.* 2008;3(2):163-175. doi: 10.1038/nprot.2007.521

34. Sathiavimal S, Vasantha Raj S, Veeramani V, et al. Green chemistry route of biosynthesized copper oxide NPs using *Psidium guajava* leaf extract and their antibacterial activity and effective removal of industrial dyes. *J Environ Chem Eng.* 2021;9(2):105033. doi: 10.1016/j.jece.2021.105033

35. Selvi JM, Murugalakshmi M, Sami P, Gnanaprakash M, Thanalakshmi R. Green synthesis, characterization and applications of TiO_2 NPs using aqueous extract of *Erythrina variegata* leaves. *Curr Sci.* 2022;123(1):59. doi: 10.18520/cs/v123/i1/59-66

36. Anbумani D, Dhandapani KV, Manoharan J, et al. Green synthesis and antimicrobial efficacy of titanium dioxide NPs using *Luffa acutangula* leaf extract. *J King Saud Univer Sci.* 2022;34(3):101896. doi: 10.1016/j.jksus.2022.101896

37. Narayanan M, Devi PG, Natarajan D, et al. Green synthesis and characterization of titanium dioxide NPs using leaf extract of *Pouteria campechiana* and larvicidal and pupicidal activity on *Aedes aegypti*. *Environ Res.* 2021;200:111333. doi: 10.1016/j.envres.2021.111333

38. Thakur BK, Kumar A, Kumar D. Green synthesis of titanium dioxide NPs using *Azadirachta indica* leaf extract and evaluation of their antibacterial activity. *S Afr J Bot.* 2019;124:223-227. doi: 10.1016/j.sajb.2019.04.003

39. Ahmad W, Jaiswal KK, Soni S. Green synthesis of titanium dioxide (TiO_2) NPs by using *Mentha arvensis* leaves extract and its antimicrobial properties. *Inorg Nano-Metal Chem.* 2020;50(10):1032-1038. doi: 10.1080/24701556.2020.1760841

40. Subhapriya S, Gomathipriya P. Green synthesis of titanium dioxide (TiO_2) NPs by *Trigonella foenum-graecum* extract and its antimicrobial properties. *Microp Pathog.* 2018;116:215-220. doi: 10.1016/j.micpath.2018.01.027

41. Huq MA, Ashrafuddoula M, Rahman MM, Balusamy SR, Akter S. Green synthesis and potential antibacterial applications of bioactive silver NPs: A review. *Polymers.* 2022;14(4):742. doi: 10.3390/polym14040742

42. Arora A, Singh K, Nagda V, Kumar D. Phytochemical screening and *in vitro* antimicrobial study of *Prosopis cineraria* L. bark. *South Asian Journal of Experimental Biology.* 2023;13(1):6-11. doi: 10.38150/sajeb.13(1).p6-11

43. Garcia-Marin LE, Juarez-Moreno K, Vilchis-Nestor AR, Castro-Longoria E. Highly antifungal activity of biosynthesized copper oxide NPs against *Candida albicans*. *Nanomaterials.* 2022;12(21):3856. doi: 10.3390/nano12213856

44. Abdel-Maksoud G, Abdel-Nasser M, Hassan SED, Eid AM, Abdel-Nasser A, Fouada A. Biosynthesis of titanium dioxide NPs using probiotic bacterial strain, *Lactobacillus rhamnosus*, and evaluation of their biocompatibility and antifungal activity. *Biomass Conv Bioref.* 2023;1-23. doi: 10.1007/s13399-023-04587-x

45. Punjabi K, Mehta S, Chavan R, Chitalia V, Deogharkar D, Deshpande S. Efficiency of biosynthesized silver and zinc NPs against multi-drug resistant pathogens. *Front Microbiol.* 2018;9:2207. doi: 10.3389/fmicb.2018.02207

46. Ali OM, Hasanin MS, Suleiman WB, Helal EEH, Hashem AH. Green biosynthesis of titanium dioxide quantum dots using watermelon peel waste: Antimicrobial, antioxidant, and anticancer activities. *Biomass Conv Bioref.* 2024;14:6987-6998. doi: 10.1007/s13399-022-02772-y

47. Al Masoudi LM, Alqurashi AS, Abu Zaid A, Hamdi H. Characterization and biological studies of synthesized titanium dioxide NPs from leaf extract of *Juniperus phoenicea* (L.) growing in Taif Region, Saudi Arabia. *Processes.* 2023;11(1):272. doi: 10.3390/pr11010272

48. Hu C, He S, Lee YJ, et al. Live-dead assay on unlabeled cells using phase imaging with computational specificity. *Nat Commun.* 2022;13(1):713. doi: 10.1038/s41467-022-28214-x

49. Kumar SSD, Houreld NN, Kroukamp EM, Abrahamse H.

Cellular imaging and bactericidal mechanism of green-synthesized silver NPs against human pathogenic bacteria. *J Photochem Photobiol B Biol.* 2018;178:259-269. doi: 10.1016/j.jphotobiol.2017.11.001

50. Sabapathi N, Ramalingam S, Aruljothi KN, Lee J, Barathi S. Characterization and therapeutic applications of biosynthesized silver NPs using *Cassia auriculata* flower extract. *Plants.* 2023;12(4):707. doi: 10.3390/plants12040707